

1 Earthquake recurrence time and patterns of forerunning earthquakes for 2 selected subduction and collision zones

3 Venkata Kambala¹, Piotr Senatorski¹,

4 ¹ Institute of Geophysics, Polish Academy of Sciences, ul. Ks.Janusza 64, 01-452 Warsaw, Poland
5 Email: vkambala@igf.edu.pl

6 **Abstract.** We analyze various data from selected subduction and collision zones, including Japan and Hima-
7 laya-Nepal regions. In the first case, we estimate the expected recurrence times of large earthquakes within a
8 given magnitude range as functions of the Gutenberg-Richter's b values, for a given geodetic moment accu-
9 mulation rate. It is argued, that the b value is related to rupture propagation conditions and asperity distribution,
10 whereas the geodetic moment rate is controlled by the seismic moment budget derived from seismic and geo-
11 detic data. In the second case, we reveal the seismicity patterns and underlying asperity structures by using
12 topological data analysis methods. In particular, we create graphs representing the forerunning earthquakes.
13 We use the graph characteristics to distinguish among different seismicity patterns and scenarios. We argue
14 that changes of these characteristics in time and space can be used for the task of seismicity forecasting.

15 **Keywords:** Earthquake forecasting, Gutenberg-Richter law, Recurrence time, Asperities, Forerunning earth-
16 quakes.

17 1 Introduction

18 Seismicity can be perceived as a stress accumulation-release process, in which the slow tectonic loading due
19 to the relative plate movement is accommodated by alternating slow and fast slips along the plate interface. The
20 asperity fault model describe the process [1,2]. It can also be described using statistics. To estimate the recurrence
21 time of large earthquakes, we combine both views. Following the method proposed by Molnar [3] and applied to
22 recent data by Avouac [4], we derive expression for earthquake recurrence times as a function of Gutenberg-
23 Richter's b value. We obtain, however, more general expressions for the full range of b values, including $b \geq 1.5$.
24 They enable us to estimate the recurrence times of earthquakes with magnitudes within a specific range Δm below
25 the assumed maximum magnitude value, m_M , if the geodetic moment rate, \dot{M}_G , is given.

26 Two examples of the Nepal-Himalaya and Japan seismicity illustrate the proposed method of recurrence time
27 and maximum magnitude estimation for a given region.

28 2 Methods

29 **Recurrence time.** The number of earthquakes with magnitudes greater or equal to m that occur in a given region
30 and time period T is given by the Gutenberg-Richter law. It can be expressed as exponential pdf for magnitude,

$$31 \quad p(m) = b' \exp[-b'(m - m_T)] / (1 - \exp[1 - b'(m_M - m_T)]) \quad (1)$$

32 where the magnitude range is $m \in \langle m_T, m_M \rangle$, and $b' = b \ln 10 = 1 / \langle m_M - m_T \rangle$ defines the mean magnitude
33 value [5]. For $b = 0$, the distribution is uniform,

$$34 \quad p(m) = 1 / (m_M - m_T). \quad (2)$$

35 The pdf can be expressed in terms of seismic moment, M_O , by using the expression

36
$$m = \log_{10}(M_O/10^{9.05})/1.5. \quad (3)$$

37 Three different cases, $b = 0$, $b = 3/2$, and $b > 0, b \neq 3/2$, should be considered.

38 The number of all events, α , can be calculated from the expression

39
$$\alpha = \dot{M}_G \cdot T / \langle M_{SE} \rangle, \quad (4)$$

40 where $\langle M_{SE} \rangle$, is the mean seismic moment, calculated from the Gutenberg-Richter distribution expressed in terms
 41 of seismic moments, and \dot{M}_G the geodetic moment accumulation rate that involves both the plate convergence
 42 rate, V_P , and aseismic slip rate, V_{AS} . In the long term, the geodetic moment is balanced by the seismic moment,
 43 $\dot{M}_G = M_{SE}$.

44 The recurrence time of earthquakes from the seismic moment range $\langle M_O, M_M \rangle$ is

45
$$T_R = T / \left(\alpha \int_{M_O}^{M_M} p(M) dM \right), \quad (5)$$

46 which gives

47
$$T_R = (M_M - M_T) / \ln(M_M/M_O) \dot{M}_G \text{ for } b = 0, \quad (6)$$

48
$$T_R = \left(\frac{\beta}{1-\beta} \right) \left[\frac{M_M^{1-\beta} - M_T^{1-\beta}}{(M_O^{-\beta} - M_M^{-\beta}) \dot{M}_G} \right], \text{ for } b > 0 \text{ and } b \neq 3/2, \beta = 2b/3, \quad (7)$$

49 and

50
$$T_R = \ln(M_M/M_T) / (M_O^{-1} - M_M^{-1}) \dot{M}_G, \text{ for } b = 3/2. \quad (8)$$

51 Equations (6-8) enable us to calculate the recurrence time of earthquakes with seismic moments greater or equal
 52 to M_O for the assumed threshold moment, M_T , maximum moment, M_M , b value, and the geodetic moment rate,
 53 \dot{M}_G , assumed to be released by earthquakes with seismic moments from the assumed range $\langle M_T, M_M \rangle$.

54 **b value.** Earthquake rupture dynamics can be reflected by the scaling between the rupture area size and the slip
 55 deficit, $D_D = V_P T$, accumulated at a locked site,

56
$$A \propto D_D^\gamma. \quad (9)$$

57 A low γ value means that lowered stress level and higher fault roughness prevent rupture front to propagate large
 58 distances between asperities. A high γ value means that due to growing slip deficit stronger and stronger asperities
 59 fail, causing slips over larger and larger areas. Higher γ are expected before large earthquakes since the stress
 60 grow in the region due to the locked asperity.

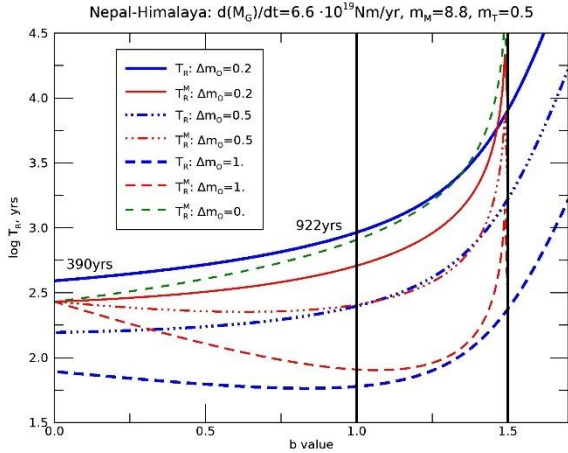
61 The Gutenberg Richter's b value can be related to γ as

62
$$b = 3/2(1 + \gamma). \quad (10)$$

63 which provides the link between earthquake statistics and fault characteristics [5,6]. For instance, $\gamma \rightarrow 0$ and $b \rightarrow$
 64 1.5 can be expected for the smallest and the largest earthquakes, where the source areas are defined by broken
 65 isolated asperities or barriers due to fault geometry or topography [6].

66 **Maximum magnitude.** Hierarchical asperity structure can be described by a forest graph of linked earth-
 67 quakes. We define earthquake closeness, which depends both on the hypocentre distance and earthquake source
 68 sizes. Then, we define forerunner earthquakes. The pairs of close earthquakes such that the larger event follows
 69 the smaller one are selected, with the earliest larger one as the only parent, and the smaller as its child or forerun-
 70 ner. The latest and largest events without parents are roots of the trees and they can be identified with asperities.
 71 The forest consisting of disjoint trees reveals the asperity fault structure. By looking at distances between the
 72 neighboring roots, we estimate magnitudes of possible future earthquakes that connect different asperities and
 73 become new roots. Such an approach can be used to define the maximum magnitude needed for the recurrence
 74 time estimation.

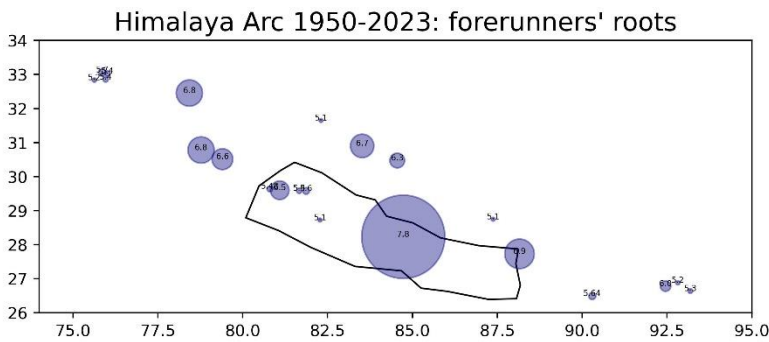
75 **3 Results**



76
77 **Fig. 1.** Earthquake recurrence time as a function of b-value for the Nepal Himalayan region. We assume that m8.8 is the
78 maximum magnitude in the region, so $M_{MAX} = 1.78 \times 10^{22}$ Nm. The threshold magnitude $m_T = 0.5$, and the moment deficit
79 mean accumulation rate $\dot{M}_G = 6.6 \times 10^{19}$ Nm/yr. The recurrence time depends on the magnitude interval $\Delta m = 0.2, 0.5, \text{ or } 1$
80 below M_{MAX} . Molnar's solutions, T_R^M , are shown for reference.

81
82 **Nepal-Himalaya.** The average convergence rate between the Indian and Eurasian tectonic plates along the 2,500-
83 kilometer-long Himalayan arc is $V_P = 20$ mm/yr. The convergence rate between India and South Tibet is
84 17.8mm/yr in central and eastern Nepal and 20.5mm/yr in western Nepal. The geodetic moment accumulation
85 rate on the Main Himalayan Thrust 1,000-kilometer-long section underneath Nepal has been estimated as $\dot{M}_G =$
86 6.6×10^{19} Nm/yr [8].

87 Recurrence times of large earthquakes are shown in Figure 1. For $b = 0$ we obtain $T_R = 390, 156, \text{ and } 78$ yrs
88 for respectively $\Delta m = 0.2, 0.5, \text{ and } 1$. For $b = 1$, $T_R = 922, 249, \text{ and } 60$ yrs the same Δm values. $b = 1.5$ seem
89 unrealistic for full magnitude range. For Molnar's (1979) solutions, $T_R \rightarrow \infty$ for $b = 1.5$. Next we consider dis-
90 tribution of 1950-2023 $m \geq 4$ earthquakes along the Himalayan Arc from the USGS catalogue. Roots of related
91 earthquake trees are shown in Figure 2. They can be thought of as representing isolated asperities. Magnitudes of
92

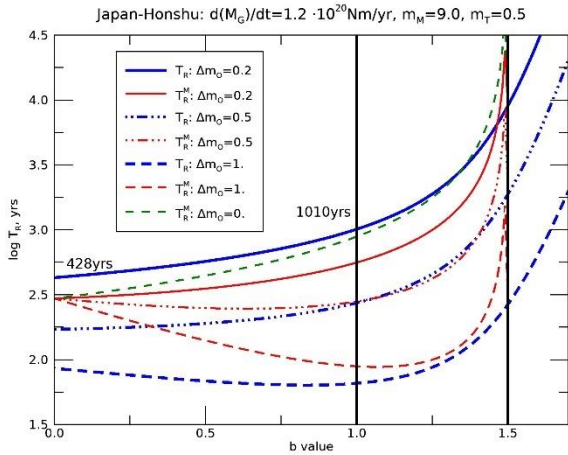


93
94 **Fig. 2.** Distribution of earthquakes 1950-2023 along Himalayan Arc. Roots of separated trees are shown only.

95
96 the future earthquakes that cover two isolated asperities can be calculated. For instance, the m8.8 earthquake is
97 needed to break both asperities related m7.8 and m6.9 roots shown in Figure 2.

98 **Honshu.** The average convergence rate between the Pacific Plate and the North American Plate is $V_P =$
 99 83mm/yr. The geodetic moment accumulation rate on the 1,000-kilometer-long section along Japan Trench has
 100 been estimated as $\dot{M}_G = 1.2 \times 10^{20}$ Nm/yr [9].

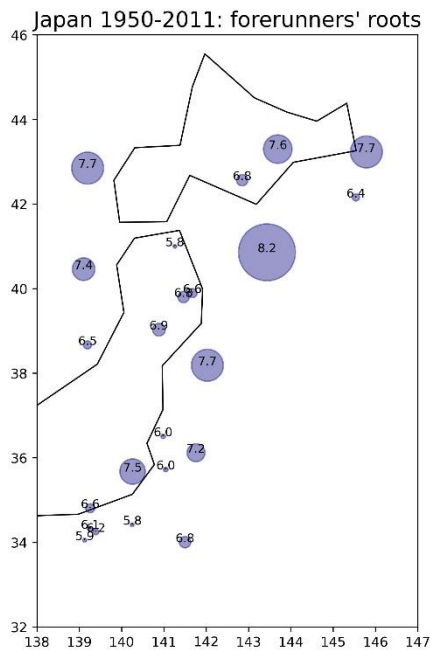
101 Recurrence times of large earthquakes are shown in Figure 3. For $b = 0$ we obtain $T_R = 428, 171,$ and 86 yrs
 102 for respectively $\Delta m = 0.2, 0.5,$ and 1. For $b = 1, T_R = 1010, 273,$ and 67 yrs for the same Δm values. Results
 103 for $b = 1.5$ seem unrealistic.



104 **Fig. 3.** Same as in Fig. 2. for Honshu region. We assume that m_9 is the maximum magnitude in the region, so $M_{MAX} = 3.55$
 105 $\times 10^{22}$ Nm.

106 Next we consider distribution of 1950-2023 $m \geq 4$ earthquakes in the Honshu region from the USGS catalogue.
 107 We focus on distances between the forerunner roots just before the largest, 2011 Tohoku-oki m_9 earthquake. For
 108 instance, $m_{8.5}$ earthquake is needed to break both asperities related $m_{7.7}$ and $m_{7.5}$ roots, and $m_{8.1}$ earthquake to
 109 break both asperities related $m_{7.5}$ and $m_{7.2}$ roots off the coast of Honshu shown in Figure 4.

110
 111
 112



113 **Fig. 4.** Distribution of earthquakes 1950-2011, before the Tohoku-oki earthquake, along Japan Trench. Roots of separated
 114 trees are shown only.
 115

116 4 Discussion

117 The asperity model assumes that the plate interface is divided into two interlocking parts, the high-coupled
118 asperities and low-coupled non-asperity regions. Asperities break singly or in groups, depending on the stress
119 level and fault roughness. They create also hierarchical structures, which suggests using their forest graph repre-
120 sentation. The weaker asperities break singly first. After the last, strongest locked site fails, the weaker sites break
121 again in larger events [2,7]. The largest m_M earthquake occurs in a given region, when all separated asperities
122 break together.

123 The b value and the maximum magnitude, m_M , are considered within the asperity model context. The Guten-
124 berg Richter's b value is related to fault characteristics, and it can depend both on time and magnitude range [5,6].
125 Here we assumed the same b value for the full magnitude range, but the method enables us divide the magnitude
126 range into intervals with different b values. A more detailed analysis should take into account the proportion in
127 which the accumulated moment deficit is released by the largest, moderate, and weak earthquakes.

128 5 Conclusions

129 Return times of strong earthquakes, estimated from the Gutenberg-Richter law, depend on three quantities:

- 130 • the rate of accumulation of geodetic moment related to the movement of tectonic plates;
- 131 • b value related to the slip propagation conditions along the contact of these plates;
- 132 • the magnitudes of the strongest possible earthquake in a given region.

133 Two examples of Nepal-Himalaya and Honshu coast regions show, how such estimates can be made from
134 available geodetic data and earthquake catalogues.

135 References

- 136 1. Lay, T., Kanamori, H., Ruff L., 1982. The asperity model and the nature of large subduction zone earthquake occurrence,
137 Earthquake Prediction Res. 1, 3-71 (1982).
- 138 2. Uchida, N., Matsuzawa, T.: Coupling coefficient, hierarchical structure, and earthquake cycle for the source area of the
139 2011 off the Pacific coast of Tohoku earthquake inferred from small repeating earthquake data. Earth Planets Space 63,
140 675-679 (2011).
- 141 3. Molnar, P.: Earthquake recurrence intervals and plate tectonics. Bull. Seism. Soc. Am. 69,115-133 (1979).
- 142 4. Avouac J-P.: From Geodetic Imaging of Seismic and Aseismic Fault Slip to Dynamic Modeling of the Seismic Cycle.
143 Annu. Rev. Earth Planet. Sci. 43, 233–71 (2015).
- 144 5. Senatorski, P.: Effect of slip-area scaling on the earthquake frequency-magnitude relationship. Phys. Earth planet. Inter.
145 267, 41-52 (2017).
- 146 6. Senatorski, P.: Gutenberg-Richter's b-value and earthquake asperity models. Pure Appl. Geophys. 177, 1891–1905 (2020).
- 147 7. Ikuta, R., Satomura, M., Fujita, A., Shimada, S., Ando, M.: A small persistent locked area associated with the 2011 Mw9.0
148 Tohoku-Oki earthquake, deduced from GPS data, J. Geophys. Res. 117, B11408, doi:10.1029/2012JB009335 (2012).
- 149 8. Ader, T. et al.: Convergence rate across the Nepal Himalaya and interseismic coupling on the Main Himalayan Thrust:
150 Implications for seismic hazard. J. Geophys. Res. 117, B04403, doi:10.1029/2011JB009071 (2012).
- 151 9. Scholz, C.H., Campos, J.: The seismic coupling of subduction zones revisited. J. Geophys. Res. 117, B05310,
152 doi:10.1029/2011JB009003 (2012).